

Tautomeric, spectroscopic, DFT calculations and X-ray studies on $\text{O}_2\text{N}-4-\text{C}_6\text{H}_4-\text{NHN}=\text{C}(\text{COCH}_3)_2$

Carlos Bustos^{a,*}, Christian Sánchez^a, Rolando Martínez^a,
 Ricardo Ugarte^a, Eduardo Schott^a, Desmond Mac-Leod Carey^b,
 María Teresa Garland^c, Luis Espinoza^d

^a Instituto de Química, Universidad Austral de Chile, Casilla 567, Valdivia, Chile

^b Departamento de Química, Pontificia Universidad Católica de Chile, Avda. Vicuña Mackenna 4860, Santiago de Chile, Chile

^c CIMAT Facultad de Ciencias Físicas y Matemáticas, Universidad de Chile, Casilla 2777, Correo 21, Santiago de Chile, Chile

^d Laboratorio de RMN, Departamento de Química, Universidad Técnica Federico Santa María, Valparaíso, Chile

Received 2 April 2006; accepted 11 April 2006

Available online 21 June 2006

Abstract

This paper deals with the structural and tautomeric studies on $\text{O}_2\text{N}-4\text{-phenyl hydrazone derivative of acetylacetone}$, of formula $\text{O}_2\text{N}-4-\text{C}_6\text{H}_4\text{NHN}=\text{C}(\text{COCH}_3)_2$, **I**, using IR, ^1H NMR and ^{13}C NMR spectroscopies, X-ray diffraction analysis and quantum mechanical calculations. The crystallographic data show that this compound has a β -diketohydrazone structure, containing an intramolecular H-bond assisted by resonance (RAHB), with $\text{N}\cdots\text{O}$ distance of 2.6025(16) Å. These results are in agreement with the spectroscopic studies and with theoretical calculations. The collected information confirms that **I** shows the same structure in CDCl_3 solution, solid state and gaseous phase.

© 2006 Elsevier Ltd. All rights reserved.

Keywords: Hydrogen bonding; Hydrazone dyes; Tautomeric studies; X-ray characterization; DFT calculations

1. Introduction

In recent years, much attention has been devoted to structural studies on heterodienic systems forming strong intramolecular hydrogen bonds, $\text{N}-\text{H}\cdots\text{O}$, assisted by resonance (RAHB) which, inter alia, could have potential technological applications as bistate molecular switches [1–6]. It is well known that the phenyl diazonium salts are capable of coupling with a series of compounds that may yield the $\text{N}-\text{H}\cdots\text{O}$ moiety. In fact, with active methylene groups of a β -diketone, such as acetylacetone [7], it has been proposed that the reaction may yield four tautomeric forms, Fig. 1: azodiketone, **a**,

β -diketohydrazone, **b**, and *E*- and *Z*-azoketoenol, **c** and **d** isomers [9], respectively. Spectroscopic studies such as UV–vis [8], IR [7] and ^1H NMR [7,8], have allowed us to discard the *E*-azoketoenol and *Z*-azoketoenol structures. Besides, using mass spectrometry fragmentation the presence of $\text{N}-\text{H}\cdots\text{O}$ bridge has been recognized [9] and the polarographic methods [10,11] have shown the presence of the electro-active group $\text{HN}-\text{N}=\text{C}$.

The purpose of this work is to provide new information to know in more detail the nature of the products formed by this coupling reaction. We have prepared compound $\text{O}_2\text{N}-4-\text{C}_6\text{H}_4\text{NHN}=\text{C}(\text{COCH}_3)_2$ (**I**) using the method described in literature [7]. Then, we carried out structural and tautomeric studies using IR, ^1H NMR, ^{13}C NMR spectroscopies and quantum mechanical calculations. The crystalline and molecular structures of **I** obtained by X-ray diffraction analysis are also discussed.

* Corresponding author.

E-mail address: cbustos@uach.cl (C. Bustos).

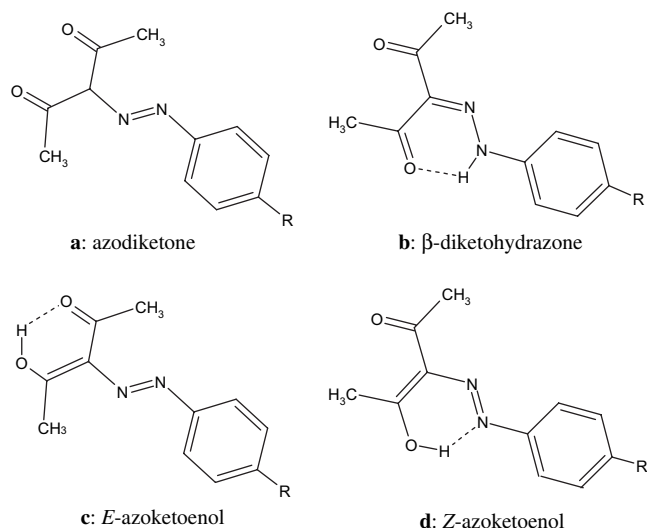


Fig. 1. A proposed structure for the coupling of diazonium salts with a β-diketetonate anion.

2. Experimental

2.1. Chemicals

4-Nitroaniline, $\text{O}_2\text{N}-4-\text{C}_6\text{H}_4-\text{NH}_2$, acetylacetone, sodium nitrite, sodium acetate, sodium hydroxide and hydrochloric acid were obtained from the usual commercial sources and used without previous purification. Solvents methanol, chloroform, toluene, and diethyl ether were dried and distilled by standard method before use.

2.2. Syntheses

2,3,4-Pentanetrione-3-[(4-nitrophenyl)hydrazone], **I**, of formula $\text{O}_2\text{N}-4-\text{C}_6\text{H}_4\text{NHN}=\text{C}(\text{COCH}_3)_2$, was prepared as described in the literature [7]. Following filtration the crude product was washed with copious quantities of hot water, dried under vacuum, recrystallized twice in toluene or chloroform and then checked by IR, ^1H NMR and ^{13}C NMR spectroscopies. Single crystals of **I** suitable for X-ray studies were obtained by diffusion of diethyl ether over a concentrated solution of CHCl_3 . Anal.: IR spectra on KBr pellet, $\bar{\nu}$ (cm^{-1}), $\bar{\nu}(\text{N}-\text{H})$: 3078 w; $\bar{\nu}(-\text{CH}_3)$: 2925 w; $\bar{\nu}(>\text{C}=\text{O}$ free): 1690 s; $\bar{\nu}(>\text{C}=\text{O}$

H-bond): 1647 s; $\bar{\nu}(>\text{CN}-)$: 1603 m; $\bar{\nu}(>\text{C}=\text{C}<)$: 1596 s. ^1H NMR in CDCl_3 , internal TMS, δ (ppm): 2.534 s (3H, free CH_3CO); 2.639 s (3H, CH_3CO in H-bond.); 7.481–7.518 m (2H, $-\text{C}_6\text{H}_4-$); 8.289–8.326 m (2H, $-\text{C}_6\text{H}_4-$); 14.537 s (1H, N–H). ^{13}C NMR in CDCl_3 , internal TMS, δ (ppm), labeled in accord to Fig. 2: C(10): 26.659; C(11): 31.848; C(1), C(5): 115.749; C(2), C(4): 125.825; C(7): 135.066; C(3): 144.601; C(6): 146.648; C(9): 196.803; C(8): 198.780.

2.3. Physical measurements

The infrared spectrum was recorded on a Nicolet FT-IR Nexus Spectrophotometer on KBr pellets. The ^1H NMR and ^{13}C NMR and HBMN spectra were recorded in CDCl_3 at 298 K on an Avance 400 Digital NMR Bruker Spectrometer, equipped with a 5.00 mm Inverse Multinuclear Detection Pulsed Field Gradients probe (^1H BBI, PFG-ZGRD, Z8202/0253), operating at 400.132 MHz and 100.623 MHz for ^1H and ^{13}C , respectively.

2.4. Data collection

Highly redundant single crystal X-ray diffraction data sets were collected at room temperature up to a max 2θ of ca. 55.76° on a Bruker AXS SMART APEX CCD diffractometer using monochromatic Mo $\text{K}\alpha$ radiation, $\lambda = 0.71069 \text{ \AA}$, and a 0.3° separation between frames. Data integration was performed using SAINT program in the diffractometer package. The structures were solved by direct methods and Fourier's difference, and refined by least squares on F^2 with anisotropic

Table 1

Crystal data and structure refinement of $\text{O}_2\text{N}-4-\text{C}_6\text{H}_4\text{NHN}=\text{C}(\text{COCH}_3)_2$, (**I**)

Empirical formula	$\text{C}_{11}\text{H}_{11}\text{N}_3\text{O}_4$
Formula weight	249.23 g/mol
Temperature (K)	295(2)
λ (Å)	0.71073
Crystal system	Monoclinic
Space group	$P2(1)/n$
a (Å)	7.0217(8)
b (Å)	12.8331(14)
c (Å)	12.7514(14)
β ($^\circ$)	97.587(2)
V (Å ³)	1139.0(2)
Z	4
$D_{\text{Calc.}}$ (g cm^{-3})	1.453
μ (mm^{-1})	0.113
$F(000)$	520
Crystal size (mm)	$0.27 \times 0.12 \times 0.03$
θ range ($^\circ$)	2.26–27.88
Index ranges	$-9 \leq h \leq 9, -16 \leq k \leq 16, -16 \leq l \leq 16$
Reflections collected	9280
Independent reflections	2551 [$R(\text{int}) = 0.0358$]
Absorption correction	None
Data/restraints/parameters	2551/0/207
Goodness-of-fit on F^2	0.874
Final indices [$I > 2\sigma(I)$]	$R1 = 0.0377, wR2 = 0.0764$
R indices (all data)	$R1 = 0.0714, wR2 = 0.0812$
$\rho_{\text{max}}/\rho_{\text{min}}$ in final ΔF (e \AA^{-3})	0.170 and -0.152
Largest diff. peak and hole	0.170 and -0.152

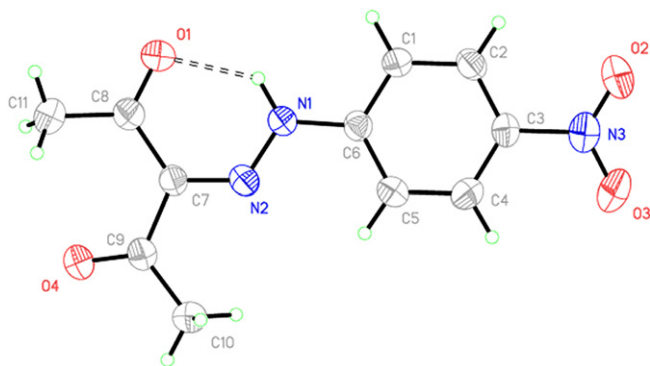


Fig. 2. Displacement ellipsoid diagram with 40% probability level of **I**. Double broken line shows the intramolecular H-bond $\text{N}(1)-\text{H}(1\text{N})\cdots\text{O}(1)$.

displacement parameters for non-H atoms. All hydrogen atoms were located from difference Fourier maps and refined isotropically. All calculations to solve the structures, to refine the model proposed and to obtain results were carried out with the computer programs SHELXS-97 and SHELXL-97 and SHELXTL/PC [13]. Crystallographic data (excluding structure factors) for the structure reported in this paper have been deposited with the Cambridge Crystallographic Data Centre as supplementary publication, CCDC No. 295833 for compound **I**. Copies of this information may be obtained free of charge from The Director, CCDC, 12 Union Road, Cambridge CB2 1EZ, UK. Fax: +44 1223 336 033. E-mail: data_request@ccdc.cam.ac.uk. Web page: <http://www.ccdc.cam.ac.uk>.

2.5. Pauling's bond orders and conjugation parameters

The π -delocalization was evaluated in terms of the Pauling's bond order [14] “ n ”, Table 5, within all the β -ketohydrazone moieties, $\text{HN}=\text{N}=\text{C}-\text{C}=\text{O}$, taking two separated subfragments, $\text{HN}=\text{N}=\text{C}$ and $\text{C}-\text{C}=\text{O}$, using as reference the

standards' single bond length in crystalline state [16] of C_2H_6 , $\text{C}-\text{C}$: 1.513 Å; CH_3OH , $\text{C}-\text{O}$: 1.413 Å; CH_3NH_2 , $\text{C}-\text{N}$: 1.469 Å and, N_2H_4 , $\text{N}-\text{N}$: 1.425 Å. These bond lengths were incorporated into Pauling's equation [14], $-\Delta R(n) = 0.353 \log n$, together with the experimental (first block) and theoretical (second block) bond lengths, $\text{C}-\text{O}$, $\text{C}-\text{C}$, $\text{C}-\text{N}$ and $\text{N}-\text{N}$, d_1-d_4 , as shown in Table 6. Simultaneously, the π -delocalization parameters, η , were evaluated in terms of percentage [12] as $\% \eta_{1,2} = 1/2[(2 - n_1) + (n_2 - 1)] \times 100$ and $\% \eta_{3,4} = 1/2[(2 - n_3) + (n_4 - 1)] \times 100$, where, $\eta_{1,2}$ and $\eta_{3,4}$ are, by definition, equal to 0, 1 and 0.5 for the non-delocalized $\text{HN}=\text{N}=\text{C}-\text{C}=\text{O}$, ionic $\text{HN}^+=\text{N}=\text{C}-\text{C}=\text{O}^-$ and fully π -delocalized $\text{HN}=\text{N}=\text{C}=\text{C}=\text{O}$ fragments, respectively. Comparisons of the crystallographic data of compounds **II–VI**, available in literature [12], were also incorporated to obtain Table 5.

2.6. Computational details

In order to know the most stable tautomeric form, a previous conformational analysis in gaseous phase using the Spartan

Table 2
Selected bond lengths (Å), angles (°) and torsion angles (°) of **I**

Bond	Length (Å)	Bond	Length (Å)
O(1)–C(8)	1.2220(16)	C(1)–C(6)	1.3839(19)
O(2)–N(3)	1.2206(15)	C(2)–C(3)	1.3769(19)
O(3)–N(3)	1.2247(16)	C(3)–C(4)	1.3728(19)
O(4)–C(9)	1.2168(15)	C(4)–C(5)	1.372(2)
N(1)–N(2)	1.3094(14)	C(5)–C(6)	1.3789(19)
N(1)–C(6)	1.3991(16)	C(7)–C(8)	1.4794(19)
N(2)–C(7)	1.3105(16)	C(7)–C(9)	1.4807(19)
N(3)–C(3)	1.4559(18)	C(8)–C(11)	1.490(2)
C(1)–C(2)	1.3701(19)	C(9)–C(10)	1.491(2)
Angle	Length (°)	Angle	Length (°)
N(2)–N(1)–C(6)	118.97(12)	C(5)–C(6)–C(1)	120.38(14)
N(1)–N(2)–C(7)	122.65(12)	C(5)–C(6)–N(1)	121.72(13)
O(2)–N(3)–O(3)	123.05(14)	C(1)–C(6)–N(1)	117.90(13)
O(2)–N(3)–C(3)	118.92(14)	N(2)–C(7)–C(8)	123.79(13)
O(3)–N(3)–C(3)	118.03(15)	N(2)–C(7)–C(9)	113.01(12)
C(2)–C(1)–C(6)	120.07(14)	C(8)–C(7)–C(9)	123.18(12)
C(1)–C(2)–C(3)	119.01(15)	O(1)–C(8)–C(7)	119.06(13)
C(4)–C(3)–C(2)	121.29(14)	O(1)–C(8)–C(11)	119.30(15)
C(4)–C(3)–N(3)	119.66(13)	C(7)–C(8)–C(11)	121.58(15)
C(2)–C(3)–N(3)	119.05(14)	O(4)–C(9)–C(7)	120.48(13)
C(5)–C(4)–C(3)	119.71(15)	O(4)–C(9)–C(10)	120.75(15)
C(4)–C(5)–C(6)	119.52(15)	C(7)–C(9)–C(10)	118.76(14)
Torsion angle	Length (°)	Torsion angle	Length (°)
C(6)–N(1)–N(2)–C(7)	178.90(12)	O(2)–N(3)–C(3)–C(4)	–165.82(14)
C(6)–C(1)–C(2)–C(3)	1.3(2)	O(2)–N(3)–C(3)–C(2)	14.5(2)
C(1)–C(2)–C(3)–C(4)	–0.4(2)	O(3)–N(3)–C(3)–C(2)	–165.80(14)
C(1)–C(2)–C(3)–N(3)	179.30(13)	O(3)–N(3)–C(3)–C(4)	13.9(2)
C(2)–C(3)–C(4)–C(5)	–0.8(2)	N(2)–C(7)–C(8)–O(1)	11.9(2)
N(3)–C(3)–C(4)–C(5)	179.49(13)	N(2)–C(7)–C(8)–C(11)	–165.38(17)
C(3)–C(4)–C(5)–C(6)	1.1(2)	C(9)–C(7)–C(8)–O(1)	16.3(2)
C(4)–C(5)–C(6)–C(1)	–0.1(2)	C(9)–C(7)–C(8)–O(1)	–166.34(14)
C(4)–C(5)–C(6)–N(1)	179.24(14)	N(2)–C(7)–C(9)–O(4)	–165.22(13)
C(2)–C(1)–C(6)–C(5)	–1.1(2)	N(2)–C(7)–C(9)–C(10)	13.7(2)
C(2)–C(1)–C(6)–N(1)	179.52(13)	C(8)–C(7)–C(9)–C(10)	–167.89(15)
N(2)–N(1)–C(6)–C(5)	–0.9(2)	C(8)–C(7)–C(9)–O(4)	13.2(2)
N(2)–N(1)–C(6)–C(1)	178.41(13)		
N(1)–N(2)–C(7)–C(8)	–2.5(2)		
N(1)–N(2)–C(7)–C(9)	175.94(11)		

Table 3
Hydrogen bonds (Å) and angles (°) present in **I**

D–H⋯A	<i>d</i> (D–H)	<i>d</i> (H⋯A)	<i>d</i> (D⋯A)	∠(D–H⋯A)
N(1)–H(1N)⋯O(1)	0.910(14)	1.900(14)	2.6025(16)	132.4(12)
C(2)–H(2)⋯O(1)#1	0.929(13)	2.519(13)	3.3983(19)	158.1(11)
C(1)–H(2)⋯O(4)#2	0.963(13)	2.479(13)	3.2146(18)	133.1(10)

Symmetry codes for the transformations: #1[$-x + 3/2, y + 1/2, -z + 1/2$]; #2[$x + 1/2, -y + 3/2, z - 1/2$].

package [15a] was carried out in Fig. 1(a–d) ($R=4\text{-NO}_2$). Then, each idealized tautomeric molecule was exported to CAChe package [15b] to perform the full geometry optimization at the B88LYP/DZVP level of theory, because, it is known that ab initio Møller–Plesset methods at MP2, MP3 and MP4 levels give substantially the same results as those obtained using the Density Functional Theory (DFT) methods BLYP [12]. Besides, we chose the DFT method due to the fact that the geometry optimizations are rather fast than the MP methods. Selected bond lengths and angles marked with (a) (footnote of Table 6) were incorporated and compared with experimental data in Table 6, second block.

3. Results and discussion

3.1. Description of the structure

Fig. 2 presents the molecular diagram of **I**, while Table 1 provides a survey of crystallographic and refinement data; Table 2 shows some selected bond distances, angles and torsion angles and Table 3 the intra and intermolecular H-bonding interactions stabilizing the structure. The structure has been well refined with final indices, [$I > 2\sigma(I)$], of $R1 = 0.0377$ and $wR2 = 0.0764$, Table 1. The relevant characteristics, Fig. 2, are (i) the presence of the β -diketohydrazone core, confirming the route followed by the coupling reaction and the tautomerization process [7]; (ii) the presence of one $\text{HN}=\text{N}=\text{C}=\text{O}$ heterodienic system with the ideal geometry to form the heteronuclear $\text{N}(1)–\text{H}(1\text{N})\cdots\text{O}(1)$ RAHB, Fig. 2, that may be considered fairly weak, Table 3 (vide infra); and (iii) the molecule is basically planar, (see torsion angles in Table 2, third block, first column), the main deviations being due to slight rotations around the $\text{C}(3)–\text{N}(3)$, $\text{C}(7)–\text{C}(8)$ and $\text{C}(7)–\text{C}(9)$ bonds (Table 2, third block, second column).

In literature [12], the crystalline structure of compounds such as $\text{Br}-2\text{-C}_6\text{H}_4\text{--NHN}=\text{C}(\text{CN})(\text{COCH}_3)$ (**II**), $\text{CH}_3\text{--}2\text{-C}_6\text{H}_4\text{--NHN}=\text{C}(\text{CN})(\text{COCH}_3)$ (**III**), $\text{CH}_3\text{O--}2\text{-C}_6\text{H}_4\text{--NHN}=\text{C}(\text{COCH}_3)(\text{CO}_2\text{CH}_3)$ (**IV**), $\text{NC--}2\text{-C}_6\text{H}_4\text{--NHN}=\text{C}(\text{COCH}_3)(\text{CO}_2\text{CH}_3)$ (**V**) and $\text{NC--}4\text{-C}_6\text{H}_4\text{--NHN}=\text{C}(\text{COCH}_3)(\text{CO}_2\text{CH}_3)$ (**VI**), that contain intramolecular $\text{N}–\text{H}\cdots\text{O}$ RAHBs with similar features to **I**, has been reported. Table 4 shows all lengths involved in the $\text{N}(1)–\text{H}(1\text{N})\cdots\text{O}(1)$ RAHBs of **I** and compounds **II–VI**. Here, it is possible to see that $\text{N}–\text{H}\cdots\text{O}$, H-bond found in **I**, with $\text{N}\cdots\text{O}$ distance, 2.6025(16) Å, falls in the middle of the $\text{N}\cdots\text{O}$ distances range, 2.550–2.660 Å, as observed in previous studies on β, β' -diketoarylhydrazones [3,4,12]. Comparatively, this suggests that the 4-NO_2 group, $\sigma_p^+ = 0.78$, located far from the $\text{N}–\text{H}\cdots\text{O}$ center, may be causing an efficient shortening of the $\text{N}–\text{H}$ distance. The two remaining intermolecular H-contacts, Table 3 and Fig. 3, are of $\text{C}–\text{H}\cdots\text{O}$ type. The one involving H(2) defines chains parallel to the *b*-axis, while the other involving H(1), links chains together into a weakly connected 3D network.

At the same time, crystalline parameters of **I** showed in Table 6 (first block) agree with the Pauling's bond orders, Table 5, where they were compared with **II–VI**. These bond orders are within the expected range for β, β' -diketoarylhydrazones [12]. Besides, all bond angles $\text{C}(6)–\text{N}(1)–\text{H}(1\text{N})$, $123.20(9)^\circ$; $\text{N}(2)–\text{N}(1)–\text{C}(6)$, $118.97(12)^\circ$; $\text{N}(2)–\text{N}(1)–\text{H}(1\text{N})$, $117.8(9)^\circ$ and $\text{N}(1)–\text{N}(2)–\text{C}(7)$, $122.66(12)^\circ$, Table 6 (first block), with the exception of $\text{N}(1)–\text{H}(1\text{N})–\text{O}(1)$, are close to 120° , showing that the $\text{N}(2)(\text{sp}^2)–\text{N}(1)(\text{sp}^2)$ union has an elevated π -character according to the 39% of π -delocalization, $\eta_{3,4}$, of the $\text{HN}=\text{N}=\text{C}$ fragment, Table 5. The low $\eta_{1,2}$ value, 16%, found for the fragment $–\text{C}=\text{C}=\text{O}$, indicates that there is some grade of free rotation specially around $\text{C}(7)–\text{C}(8)$ union, that explains the increase of the $\text{N}(1)–\text{H}(1\text{N})\cdots\text{O}(1)$ angle, towards a value different from

Table 4
Comparison of RAHBs parameters (Å and °) of compound **I** and **II–VI** reported in the literature

Compound	D–H⋯A ^b	<i>d</i> (D–H)	<i>d</i> (H⋯A)	<i>d</i> (D⋯A)	∠(DHA)
I (this work)	$\text{N}(1)–\text{H}(1\text{N})\cdots\text{O}(1)$	0.910(14)	1.902(14)	2.6025(16)	132.30(12)
I (this work) ^a	$\text{N}(1)–\text{H}(1\text{N})\cdots\text{O}(1)$	1.044	1.737	2.580	134.59
II	$\text{N}(1)–\text{H}(1)\cdots\text{O}(1)$	0.75(3)	2.01(2)	2.594(3)	135(3)
III	$\text{N}(1)–\text{H}(1)\cdots\text{O}(1)$	0.99(3)	1.76(3)	2.596(3)	140(2)
IV	$\text{N}(1)–\text{H}(1)\cdots\text{O}(1)$	0.88(2)	1.86(2)	2.560(2)	135(2)
	$\text{N}(1)–\text{H}(1)\cdots\text{O}(4)$	0.88(2)	2.32(3)	2.616(2)	99(2)
V	$\text{N}(1)–\text{H}(1)\cdots\text{O}(1)$	0.86(4)	1.96(5)	2.541(5)	124(4)
VI	$\text{N}(1)–\text{H}(1)\cdots\text{O}(2)$	0.85(3)	1.91(3)	2.615(3)	139(3)

^a Theoretical calculations.

^b The original atoms' labeling was used for **II–VI** [12].

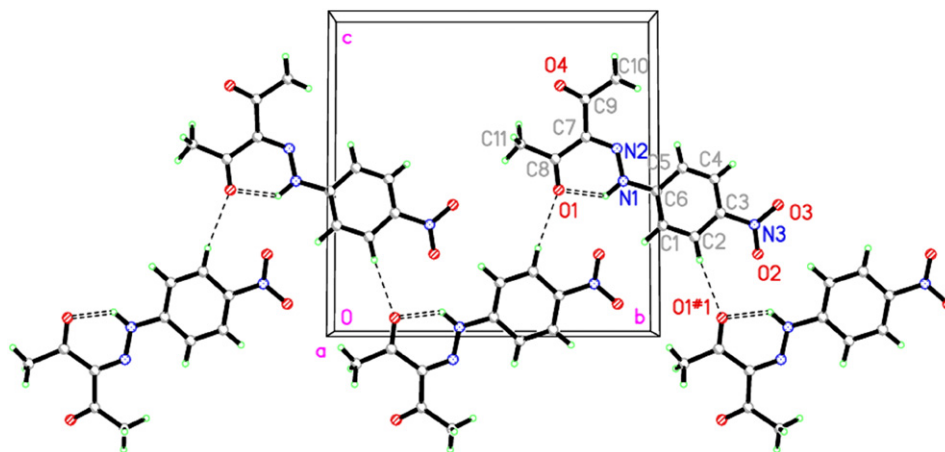


Fig. 3. Packing view of **I**, drawn along the *a*-axis and showing the chain along the [0 1 0] direction defined by the C(2)–H(2)···O(1)#1 H-bond. The second intermolecular H-bond, C(1)–H(1)···O(4)#2, (not drawn, for clarity) points upwards (downwards) defining a weakly bound 3D network.

120° (132.30(12)°, Table 4), indicating that electronic effects take priority over the steric factors involved in the RAHB.

3.2. Spectroscopic data

In CDCl₃ solution, the signals observed in the ¹H NMR and ¹³C NMR spectra of **I**, were perfectly identified with the help of HBMN spectrum (see Section 2.2). Compound **I** does not show indications of the tautomers' presence in this solvent. However, with respect to the N–H absorptions in the IR and ¹H NMR spectra, some additional considerations are required. Hydrogen bonds as short as 2.54–2.61 Å are expected to produce the N–H lengthening with respect to the undisturbed hydrogen bond found by neutron diffraction [17], 1.009 Å, or gas electron diffraction [18], 1.0116 Å. Unfortunately, X-ray diffraction is unable to locate protons' positions with sufficient accuracy. In fact, all crystallographic data fall in the much shorter range of 0.75–0.99 Å and compound **I** is not the exception, *d*(N–H): 0.0910(14) Å. However, this N–H lengthening can be appreciated in the ¹H NMR measurement in CDCl₃ solution. Weak N–H···O bonds known to give δ (N–H) values within the range of 7.0–9.0 ppm and ~15 ppm are reported for the strongest N–H···O interaction [12]. The observed value for compound **I** in CDCl₃ solution, 14.537 ppm, is a clear indication of some N–H lengthening in solution, which is confirmed by the stretching frequency value, $\bar{\nu}$ (N–H): 3078 cm^{−1}, in the IR spectrum on KBr disc. In this case, 3400 cm^{−1} has been reported for the free $\bar{\nu}$ (N–H) group and 3400–3200 cm^{−1} range for the N–H groups involved in non-resonant H-bonds. The reported data showed that the shifts may reach even close to 2950 cm^{−1} for the N–H stretching involved in strongest RAHBs [12].

3.3. Density Functional Theory calculations

Crystallographic experimental findings have been submitted to verification by DFT calculations with sufficient accuracy, using the adequate model of each tautomers, Fig. 1(a–d) (R=4-NO₂), with the appropriate structure for

discriminating among the different steric and electronic effects. The absolute energy of the four eventual tautomers formed by compound **I** increase in the order: β -diketohydrazone, **b** < *E*-azoketoenol, **c** < *Z*-azoketoenol, **d** < azodiketone, **a**, which confirms β -diketohydrazone, **b**, as the most stable structure. This agrees with the previous experimental results reported in the literature [7,9,10,12] and with the crystalline structure reported here. The distances and selected angles obtained by DFT calculations (second block) are compared with the experimental data (first block) in Table 6. Moreover, with respect to the RAHB parameters, DFT calculations of **I** show that the distance *d*(N–H), 1.044 Å is longer and *d*(O···H), 1.737 Å is shorter than the one found by crystallographic methods, 0.910(14) Å and 1.902 Å, respectively. The differences may be owed to calculations that were performed in gaseous phase. However, there is no considerable change in the distance N···O and in the angle N–H···O and both parameters fall within the range expected for this variety of compounds [12], Table 4. Finally, Pauling's bond orders, *n*, and conjugation parameters, η , of the idealized structure also agree with the experimental data presented here and with those available in literature [12], Table 5.

4. Conclusions

The crystalline and molecular structures of a β -diketohydrazone, O₂N-4-C₆H₄-NHN=C(COCH₃)₂, prepared by

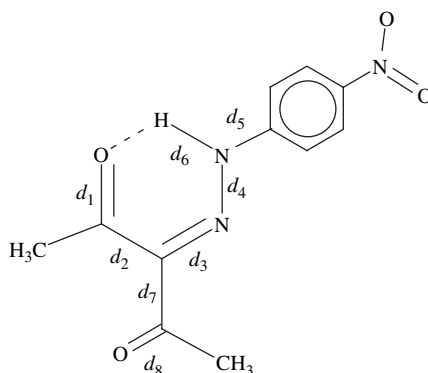
Table 5

Pauling's bond order, *n*, and π -delocalization parameters, η , of **I** compared with compounds **II**–**VI** [12]

Compound	<i>n</i> ₁	<i>n</i> ₂	<i>n</i> ₃	<i>n</i> ₄	% η _{1,2}	% η _{3,4}
I (this work)	1.87	1.18	1.68	1.46	16	39
I (this work) ^a	1.64	1.09	1.51	1.35	22	42
II	1.91	1.10	1.64	1.50	10	43
III	1.79	1.17	1.49	1.52	19	52
IV	1.82	1.11	1.57	1.52	14	48
V	1.84	1.10	1.59	1.55	13	48
VI	1.92	1.07	1.72	1.45	8	36

^a Theoretical calculations.

Table 6

Comparison of some experimental bond lengths and angles of **1** with the respective theoretical^a data

Bond lengths (Å)			Angles (°)	
d_1	O(1)–C(8)	1.2219(16)	O(1)–C(8)–C(7)	119.06(13)
d_2	C(7)–C(8)	1.4794(19)	N(2)–C(7)–C(8)	123.78(13)
d_3	N(2)–C(7)	1.3106(16)	C(6)–N(1)–H(1N)	123.2(9)
d_4	N(1)–N(2)	1.3092(15)	N(1)–N(2)–C(7)	122.66(12)
d_5	N(1)–C(6)	1.3991(16)	N(2)–N(1)–C(6)	118.97(12)
d_6	N(1)–H(1N)	0.910(14)	N(2)–N(1)–H(1N)	117.8(9)
d_7	C(7)–C(9)	1.4808(19)	C(8)–C(7)–C(9)	123.19(12)
d_8	O(4)–C(9)	1.2169(15)	N(2)–C(7)–C(9)	113.01(12)
Bond lengths ^a (Å)			Angles ^a (°)	
d_1	O(1)–C(8)	1.2610	O(1)–C(8)–C(7)	119.02
d_2	C(7)–C(8)	1.5030	N(2)–C(7)–C(8)	123.74
d_3	N(2)–C(7)	1.3420	C(6)–N(1)–H(1N)	121.33
d_4	N(1)–N(2)	1.3320	N(1)–N(2)–C(7)	120.33
d_5	N(1)–C(6)	1.4080	N(2)–N(1)–C(6)	122.02
d_6	N(1)–H(1N)	1.0440	N(2)–N(1)–H(1N)	116.56
d_7	C(7)–C(9)	1.5080	C(8)–C(7)–C(9)	121.96
d_8	O(4)–C(9)	1.2420	N(2)–C(7)–C(9)	114.29

^a Theoretical calculations.

coupling reaction between the diazonium salt and the acetylacetonate anion are shown in this study. In addition, this compound contains a heteronuclear, N–H···O, RAHB. The absolute energy of the four eventual tautomers formed by this compound determined by DFT calculations confirms β -diketohydrazone as the stablest and only product yielded by the coupling reaction. The X-ray diffraction, spectroscopic methods, IR and NMR, and DFT calculations show that the studied compound presents the same β -diketohydrazone structure in solid and gaseous phases and also in chloroform solution. Finally, the presence of one heterodienic system, HN–N=C–C=O, forming a fairly weak heteronuclear RAHB, N–H···O, has been supported by crystallographic data, which also allowed establishing that the system shows an acceptable level of π -conjugation, as supported by Pauling's bond orders, n , delocalization parameters, η , and DFT calculations. The lengthening of N–H distance was confirmed by ¹H NMR and IR spectroscopies.

Acknowledgements

The authors greatly acknowledge the financial support received from Dirección de Investigación y Desarrollo, DID-UACH, of the Universidad Austral de Chile (Grant No.

S 2003-03) and they also thank CIMAT for their permission to use the diffractometer and CCD detector.

References

- [1] Olivieri AC, Wilson RB, Paul IC, Curtin DY. *J Am Chem Soc* 1989;111:5525–32.
- [2] Inabe T. *New J Chem* 1991;15:129–36.
- [3] Bertolasi V, Ferretti V, Gilli P, Gilli G, Issa YM, Sherif OE. *J Chem Soc Perkin Trans 2* 1993;2223–8.
- [4] Bertolasi V, Nanni L, Gilli P, Ferretti V, Gilli G, Issa YM, et al. *New J Chem* 1994;18:251–61.
- [5] Bertolasi V, Gilli P, Ferretti V, Gilli G. *Acta Crystallogr Sect B* 1994;50:617–25.
- [6] Krygowski TM, Wozniak K, Anulewics R, Pawlak D, Kolodziejewski W, Grech E, et al. *J Phys Chem* 1997;101:9399–404.
- [7] Yao HC. *J Org Chem* 1964;29:2959–62.
- [8] Yagi Y. *Bull Chem Soc Jpn* 1963;36:487–92.
- [9] Carrillo D, Oliva A, León G. *Bol Soc Chil Quím* 1984;29:273–7.
- [10] Malik W, Goyal RN, Mahest VK. *Electroanal Chem* 1975;62:451–8.
- [11] Kitaev YP, Budnikov GK, Maslova L. *Izv Akad Nauk SSSR Ser Khim* 1967;9:1906–11.
- [12] Bertolasi V, Gilli P, Ferretti V, Gilli G, Vaughan K. *New J Chem* 1999;23:1261–7.
- [13] (a) Sheldrick GM. *SHELXTL-PC*. Version 5.03. Madison, Wisconsin, USA: Siemens Analytical X-ray Instruments Inc.; 1994;

- (b) Sheldrick GM. SHELXS97 and SHELXL97. Germany: University of Göttingen; 1997.
- [14] Pauling L. *J Am Chem Soc* 1947;69:542–53.
- [15] (a) Wavefunction, Inc., 18401 Von Karman Avenue, Suite 370, Irvine, CA 92612, USA; 2005.
(b) CAChe Group. Fujitsu, 1250 E, Arques Avenue, Sunnyvale, CA 94085, USA; 2002.
- [16] Lide DR. *Handbook of chemistry and physics*. 80th ed. Boca Raton, London, New York, Washington, DC: CRC Press; 1999–2000. p. 1–11, Section 9.
- [17] Allen FH, Kennard O, Watson DG, Brammer G, Orpen G, Taylor R. *J Chem Soc Perkin Trans 2* 1987:S1–19.
- [18] Vilkov LV, Sadova NI. Stereochemical applications of gas-phase electron diffraction. In: Hargittai I, Hargittai M, editors. Weinheim: VCH; 1988. Part B: p. 36–92 [John Wiley & Sons Inc.].